PROBABILISTIC COMPARISON OF DESTRUCTIVE RE-ENTRY TOOLS

James Beck[(1)], Ian Holbrough[(1)], Jim Merrifield[(2)], Stijn Lemmens[(3)]

[(1)] Belstead Research Limited, 387 Sandyhurst Lane, Ashford, TN25 4PF, UK, Email:{james.beck, ian.holbrough}@belstead.com
[(2)] Fluid Gravity Engineering Ltd., 1 West Street, Emsworth, PO10 7DX, UK, Email:jim.merrifield@fluidgravity.co.uk
[(3)] ESA-ESOC, Robert-Bosch-Straße 5, 64293 Darmstadt, Germany, Email:Stijn.lemmens@esa.int

ABSTRACT

Recently, ESA have developed a framework in which a probabilistic assessment of destructive re-entry can be performed. This framework, known as PADRE, considers uncertainties to atmospheric density, aerothermodynamic heating and aerodynamic drag, material properties, fragmentation modelling and initial conditions within a Monte Carlo assessment. Sensitivities to the aerothermodynamic heating and fragmentation were found to be dominant, with significant contributions from uncertainties in melt temperature for alloys with low melt temperatures and in emissivity for alloys with high melt temperature.

The PADRE software has been developed to be tool agnostic, and adapters have been constructed for a number of destructive re-entry codes. The tool comparison in this paper is performed between ESA's DRAMA suite, the baseline tool for risk assessments for ESA spacecraft, and the SAMj destructive re-entry research code, which has some useful verification from ground test rebuilding. Both of these tools employ a component-based spacecraft model, where the spacecraft is constructed of a set of primitive components linked by joints.

1 INTRODUCTION

The high levels of uncertainty associated with the analysis of destructive spacecraft re-entry, fragmentation and demise are well known. It has also been observed that there is significant variation in the results produced by the different re-entry verification and analysis tools in a number of different studies [1, 2].

The difficulties in obtaining a reliable result complicates mission planning and the adoption of risk mitigation measures advocated by design-for-demise as the uncertainty in the casualty risk assessment is large. Uncertainties are not consistent through the development lifecycle as more complex tools with different models are often used later in the development process, and these have a different uncertainty profile.

In addition to this, recent testing has demonstrated that a number of the material and modelling assumptions which were prevalent in the codes are in error, and different models have been proposed. Particular issues have been found in the low values of material emissivity used for metallic materials where the data suggests significantly higher emissivities of oxidised surfaces should be used [3, 4], and in the later failure of aluminium materials due to molten metal being contained within a robust oxide bag, such that failure on reaching melt temperature is not an appropriate model [5].

In order to make an assessment of the uncertainties, and to provide a set of modelling best practices, the ESA PADRE tool has been constructed [6]. This uses a probabilistic model based on a comprehensive review of the variables which drive spacecraft demise. As part of the development of the PADRE tool, a common input format has been defined using a simple excel spreadsheet template. As PADRE is re-entry code agnostic, this allows direct comparison of any re-entry software tool where a suitable adapter is written. Currently adapters exist for DRAMA, SAMj and the CNES DEBRISK tool.

This provides an opportunity to perform more in-depth comparison of the destructive re-entry codes as the common input format ensures that the same model is used in all tools, and the probabilistic nature of the comparison provides a broader view of the demise response which cannot be obtained from a single run.

2 PROBABILISTIC FRAMEWORK

The baseline model for the PADRE input uncertainties is given in Tab. 1. It is worth noting that the ±30% on the continuum aerothermodynamic heating is considered to be applicable for simple shapes, and that more complex shapes, where shock interaction and cavity effects can be important, may be higher. It is also worth noting that this uncertainty is applicable to 3dof, tumble-averaged values, with the uncertainties at specific orientations and locations being significantly higher. This observation is also true for the aerodynamic forces. This is important, as a sensitivity analysis has shown that the aerothermodynamic heating is a key driver of the demisability. This has implications for the representation of equipment in the simplified destructive re-entry tools.

Testing has also suggested [7] that the heating is driven

by local length scales rather than global length scales. This has implications for tools which construct a spacecraft geometry from primitive shapes, such as SAMj and DRAMA, and for panel-based tools such as SCARAB and PAMPERO. Both SAMj and DRAMA employ local length scale based heating models.

Table 1: Baseline Input Uncertainties

Uncertainty	Approximate Errors	Comments
Aerodynamic drag Continuum	10% uniform	Could be systematically low for slender objects at low AoA
Aerodynamic drag and heating, Free molecular	10% uniform	Errors introduced by speed ratio and mutual shading
Heat Flux Continuum	30% uniform	Still very limited data available with which to make assessment. 30% is a conservative estimate
Transitional drag and heating	±50% on characteristic length scale used for Knudsen number definition, uniform	Provide reasonable variation in transitional heating and aerodynamics whilst remaining continuous
Oxidised Emissivity	±25%, triangular. Maximum does not exceed 1	Based on data from [2]
Specific heat capacity	±5% normal three sigma limit	Effect likely to be insignificant wrt heating uncertainty
Latent heat of melt	±5% normal three sigma limit	Effect likely to be insignificant wrt heating uncertainty
CFRP thermal diffusivity	$2x10^{-8}$– $4x10^{-7}$ J/m^3K uniform distribution	Initial fit to plasma wind tunnel data
Alloys melt temperature	±30 K uniform	Capture non-eutectic effects
Atmospheric density	±10% normal one sigma	Based on seasonal variations

A set of uncertainties for joint failures has also been constructed, although the majority of the fragmentation events which have been observed in tests [8], and are modelled in SAMj, are not modelled in other tools. In this work, therefore, a six-degree-of-freedom (6dof) SAMj run was used to calibrate the fragmentation modelling. Initially, application of the test results produced high fragmentation altitudes, which were higher than those which have been observed, and so a more conservative bridging function for the aerothermodynamic heating was used in SAMj in order to reduce the fragmentation altitudes predicted. For consistency, this bridging function was used throughout the SAMj simulations.

As a result of this, the SAMj simulations used a melt fraction of aluminium (0.7±0.2) for fragmentation, and the DRAMA simulations used fragmentation at melt onset. This difference was driven by lower heating of the DRAMA model to the compound object which was traced to a visibility issue which has since been fixed. Thus later versions of DRAMA will provide different results.

As well as the physical uncertainties, the uncertainties in the modelling were also considered, and it was determined that the complexity of the spacecraft equipment, and the simplicity of the models was sufficient to result in the interpretation of the engineer in constructing the model to be a dominant factor in the results produced. This increases the importance of the definition of modelling best practices and guidelines such as ESA's DIVE [9].

A number of statistical models were investigated within PADRE. The complexity of the spacecraft model and the non-linearity of the re-entry problem resulted in a basic Monte Carlo being the most appropriate approach.

3 RE-ENTRY TOOLS

The two destructive re-entry tools considered in this comparison are DRAMA and SAMj. These tools are the two major codes based on the concept introduced in [10] where a spacecraft is constructed from a set of primitive shapes connected by joints.

DRAMA (version 3.0.2 is used here) is ESA's baseline destructive re-entry tool for spacecraft casualty risk analysis. It uses the concepts of 'contained-in' to provide nested modelling, and 'connected-to' to allow multiple primitive objects to be connected at the same level.

The aerodynamics and aerothermodynamics of individual primitives are calculated from pre-computed attitude-dependent databases, and combined using a voxelator method to account for shading.

DRAMA runs a tumble-average (or specific attitude) model for both forces and heating, performing the trajectory in 3dof. Heating is performed using a bulk heating model for all materials, with a 1D model implemented for CFRP. A code schematic is given in Fig. 1.

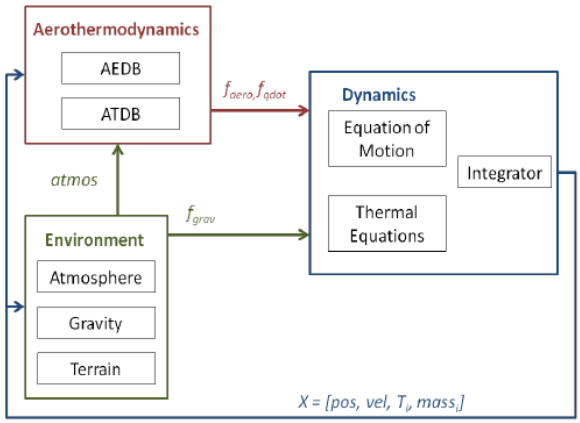

Figure 1. DRAMA System Context (from [11])

The SAMj destructive re-entry code is a collaborative development between Belstead Research and Fluid Gravity Engineering which makes use of an integrated Java / JavaScript framework. This integrated toolset comprises eight modules, which may be used individually or in combination as shown in Fig. 2.

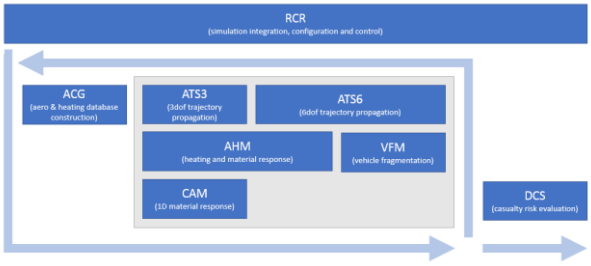

Figure 2. SAMj Framework

RCR combines the other modules to provide an integrated probabilistic engineering assessment of the on-ground casualty risk from a destructive re-entry. The ATS3 and ATS6 modules are high performance 3dof and 6dof trajectory codes.

AHM is the aerothermal heating module. It can be linked to ATS3/6 to provide the aerothermodynamic heating and material thermal response along a trajectory, or it can be used to simulate the conditions in a wind tunnel. The thermal response can be bulk heating, a simplified Heat Balance Integral (HBI) or a one-dimensional conduction/ablation model (CAM) can be embedded.

VFM evaluates the break-up of complex geometries, based on melt fraction, aerodynamic and heat loading. The fragmentation criteria used are based on available experimental data, rather than simple modelling assumptions.

ACG is a 6 degree of freedom vehicle drag and heating coefficient evaluation code and is implemented using rays cast from the panels to generate shaded drag and heating coefficients. It also contains a number of state-of the-art correlations for primitive shapes, inclusive of rings and frustums, which account for flow properties such as stream-length, and a unique mechanism for combining these correlations into heating profiles for compound shapes. It also calculates casualty areas of compound shapes using convex hulls.

A number of useful aspects are common to both tools. Databases for each geometric configuration are stored, providing increased efficiency for Monte Carlo calculations as repeat geometries occur regularly in the fragmentation process.

4 TEST CASES

Four spacecraft have been modelled for use in this work, with the data having been provided by the manufacturers. The modelling of the spacecraft has been performed in a manner which is suitable for DRAMA3 and SAMj inclusive of object location, orientation and connections, and has been implemented via the common input format.

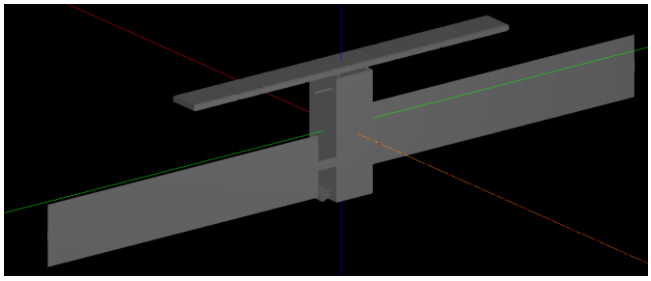

Figure 3: Sentinel-1 Model

The first two spacecraft are shown in Figs. 3 and 4. The external views shown do not demonstrate the full complexity of the models, which comprise a total of 139 and 201 geometric primitives respectively.

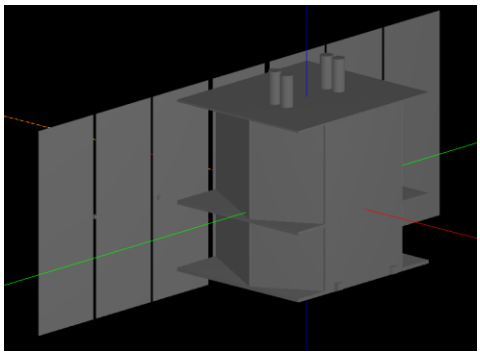

Figure 4: BeppoSax Model

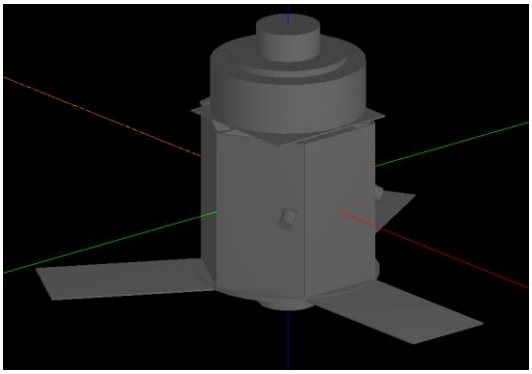

Figure 5: AstroBus Model

The remaining spacecraft selected are a generic AstroBus platform with an optical payload and electric propulsion, and a Sentinel-2 like model with the ceramic optical elements replaced by CFRP, invar, zerodur and titanium parts to provide more marginally demisable elements for the probabilistic study. Note that the material models are identical in both tools, with the exception of CFRP where each tool uses its native model due to the significant differences in the more complex material model. These models are shown in Figs. 5 and 6.

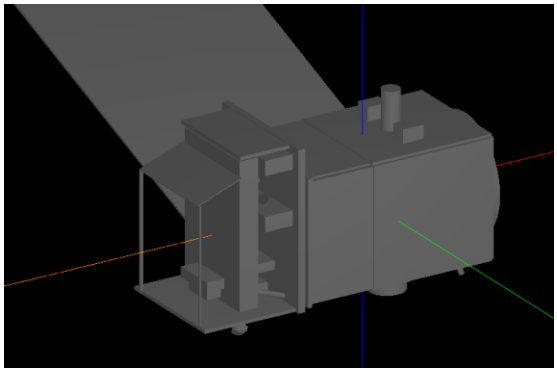

Figure 6: Sentinel-2-like Model

Again, the complexity of the internal parts is not fully seen, with the AstroBus and Sentinel-2 models comprising 151 and 134 primitives respectively. This complexity is demonstrated for the AstroBus model in Figure 7, and the Sentinel-2-like model in Figure 8.

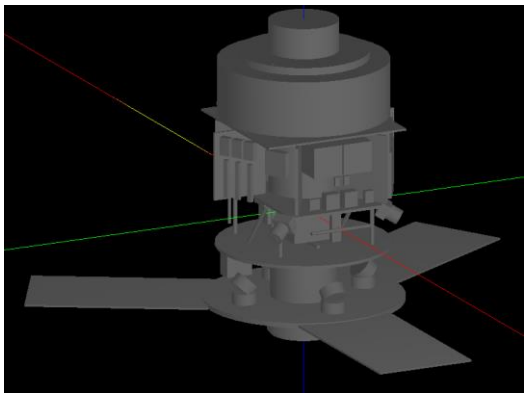

Figure 7: AstroBus Internals

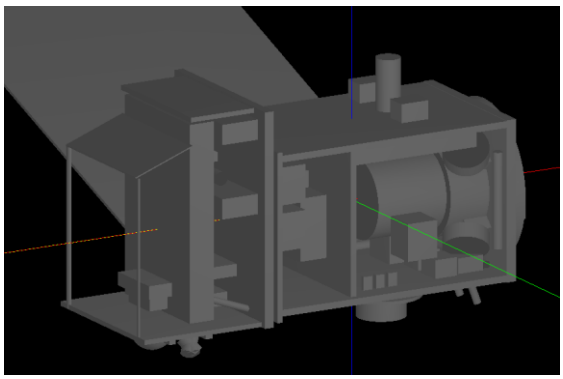

Figure 8: Sentinel-2-like Internals

As well as the four different spacecraft, four different re-entry types are also assessed. Controlled and semi-controlled re-entry from decaying circular orbits, controlled re-entry from 800km, and a high-speed interplanetary re-entry have been used. Uncertainties for each of the initial conditions has been considered. For the uncontrolled re-entry from a decaying circular orbit, it has been found that reliable results are obtained by using a random true anomaly on a 130km circular orbit as the initial condition uncertainty. This initial condition approach is recommended for application in future probabilistic studies.

5 RESULTS COMPARISON

Each of the test cases has been run using the Monte Carlo option within PADRE, with a maximum number of 5000 simulations. Generally, convergence is dependent upon gaining sufficient statistics for objects which land very occasionally, and all the macroscopic data is well converged in all cases.

The mean spacecraft mass fraction which reaches the ground in the uncontrolled re-entry cases is shown in Fig. 9. The mean mass is less than 20% of the original spacecraft mass in all cases, with the agreement between the tools being good. The largest difference is seen for the Sentinel-2 spacecraft, and this is due to the CFRP model used for the optical bench and surrounding structure. In SAMj, this material is low demise, but can fail, whereas in DRAMA, the material is essentially undemisable. The landed mass fraction of Sentinel-1 is low in both tools, with SAMj landing about 40% less mass than DRAMA. The results for BeppoSax and AstroBus are in very good agreement.

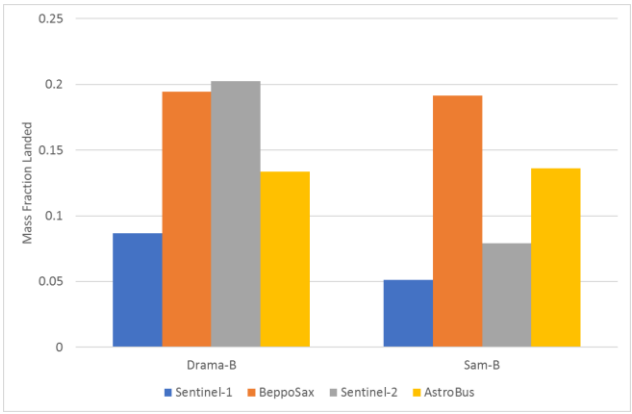

Figure 9. Mean Landed Mass in Uncontrolled Re-entry Cases

The mean number of landed objects in each case is shown in Fig. 10. Again, the general agreement can be seen to be good, particularly for AstroBus. This is due to the nature of the spacecraft components, which both codes tend to predict as always demising, or never demising. SAMj shows a higher number of landed objects for both Sentinel-1 and BeppoSax. The Sentinel-1 landed objects are dominated by small fragments from the Synthetic Aperture Radar (SAR) panel.

It is also worth noting that a model has been used for electronics GFRP cards based on the tests of [7]. This has been shown to be highly resistant to demise. As this provides a significant number of landed objects, this model requires further assessment before it can be recommended for use in risk assessments more generally.

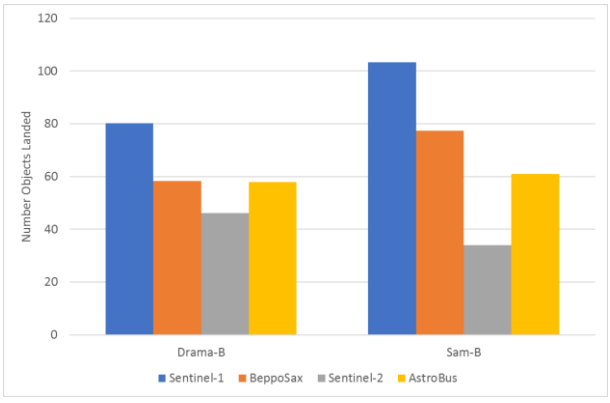

Figure 10. Mean Number of Landed Objects in Uncontrolled Re-entry Cases

The number of landed objects is high compared with the majority of previous studies, where the number of landed objects reported tends to be of the order of 10 [1, 12].

That this higher number of objects is in generally good agreement between the two tools suggests that this is legacy of the spacecraft modelling rather than the particular tool used. Care has been taken in the model construction to capture as many potentially demise-resistant parts as possible, within nested models where necessary. It is also the case that up-to-date material models have been employed, and these have higher emissivities for the majority of materials, which reduces demise. Further, the aluminium alloy specific heat capacity has been substantially underestimated in a number of previous works [13, 14].

With the landed mass being consistent, or perhaps low, in relation to previous studies, but the landed fragment count being substantially higher, this suggests that the mean mass per landed object is relatively small. This is indeed the case, as is shown in Fig. 11. Mean fragment masses of a few kilograms are predicted by both tools, with SAMj tending to predict slightly smaller objects. This is consistent with the tendency of SAMj to predict slightly smaller landed masses and slightly higher landed object numbers than DRAMA.

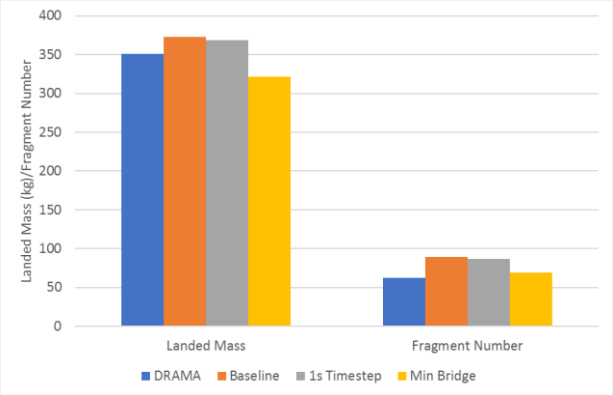

Figure 11. Mean Mass of Landed Objects from Uncontrolled Re-entries

The extension of this assessment to the other re-entry types is shown in Fig. 12. Note that a controlled re-entry case was performed for only three spacecraft, with BeppoSax being used uniquely for a high-speed interplanetary re-entry test case. This test case can immediately be seen to provide a high energy re-entry condition in which a significantly higher fraction of the spacecraft mass is demised. With the re-entry being at 12km/s and a -12^0 flight path angle, this is a significantly different case from a controlled re-entry from Low Earth Orbit (LEO).

The controlled re-entries tend to show an increased landed mass relative to the uncontrolled re-entries. Although this is not distinct in all cases, the higher energy of the controlled re-entry is, unlike the interplanetary re-entry, not sufficient to offset the shorter re-entry time. This results in the overall heat load to the spacecraft being lower, and thus the demise is lower than for an uncontrolled re-entry.

Of note is the agreement between the tools that an uncontrolled re-entry and a semi-controlled re-entry, which is controlled to 120km, are essentially the same in terms of demise. This finding is consistent across all the spacecraft.

Again, the demise behaviour of the AstroBus spacecraft is very consistent between the tools, and the re-entry types, suggesting that there is a very clear distinction between spacecraft components which are demisable and those which are not. This is the type of assessment which is much clearer with a probabilistic approach, as the insensitivity to variations cannot be determined from a limited number of simulations.

Consistently with the findings from the uncontrolled re-entry case, SAMj lands a smaller mass than DRAMA in the Sentinel-1 and Sentinel-2 cases, with the CFRP modelling again being the key driver in the Sentinel-2 case.

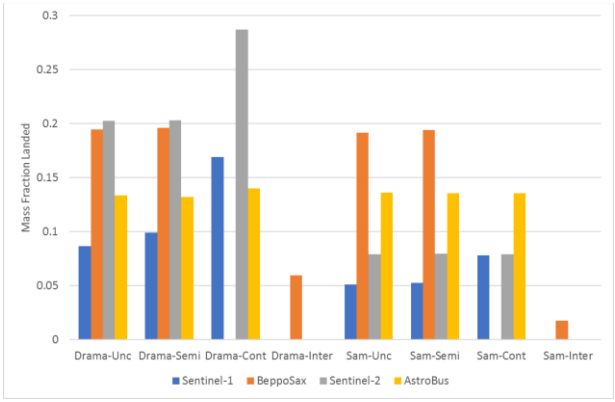

Figure. 12. Mass Fraction Landed Across Different Re-entry Types

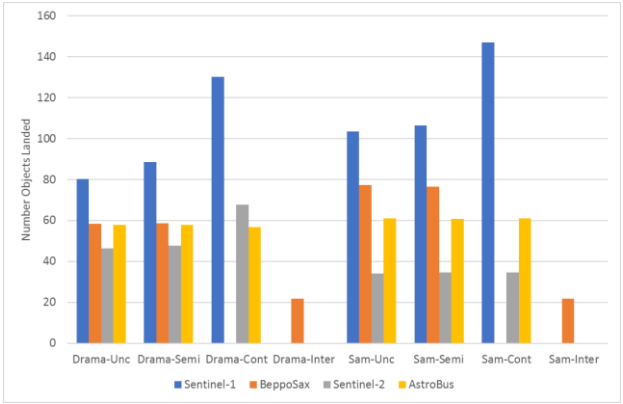

Figure 13. Landed Fragment Number Across Different Re-entry Types

The landed fragment number across the different re-entry types is shown in Fig. 13. This consolidates the agreement between the uncontrolled and semi-controlled cases, and the high demise observed in the interplanetary

case. Consistently with the observations on the uncontrolled case, SAMj appears to land slightly more objects than DRAMA across the different re-entry types.

The fragment numbers landed are again high relative to previous work, but the consistency between the tools consolidates the assertion that this occurs as a result of the modelling rather than the behaviour of a particular re-entry tool.

Given the consistency of the observation that SAMj lands a lower mass than DRAMA, but a higher fragment number, an investigation into this behaviour was performed. The demise methodology in SAMj is a forward prediction of the terminal velocity of the fragment in its current state, assessing whether this provides a 15J impact energy at the current mass. SAMj also uses an algorithm to reduce the area of a demising primitive object relative to the mass loss. It does this in proportion to the area/volume reduction of a solid sphere in order to avoid the overprediction of ballistic coefficient reduction as an object demises. DRAMA demises objects through complete mass loss, energy of the current object below 15J and ballooning, where an object is not allowed to become unphysically thin.

With the timestep in DRAMA being 1s as default, which is significantly longer than the 0.01s used in SAMj, it was thought that this was likely to be the reason that greater demise was seen in DRAMA. The hypothesis was that the shorter timestep allowed the trajectory to capture the reduction in the ballistic coefficient more accurately, such that the demise rate reduced and the object was more likely to survive. The findings on the BeppoSax satellite are shown in Fig. 14, and clearly demonstrate that increasing the timestep to 1s in SAMj has a small, but insufficient effect.

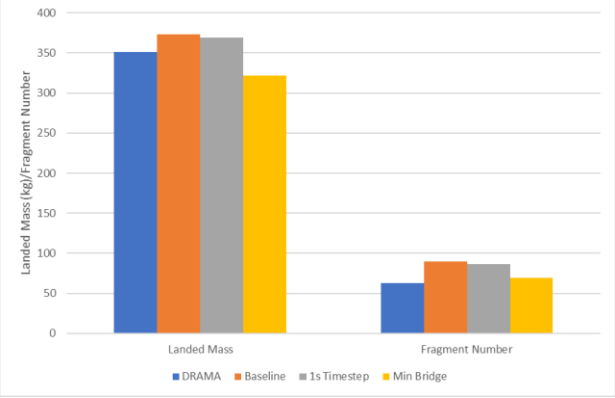

Figure 14. Impact of Timestep and Bridging Function

As the timestep difference was determined not to be the reason for the discrepancy, other hypotheses were made. It was noted earlier that the aerothermodynamic bridging function used in SAMj was changed from the default bridge (minimum of continuum and free molecular heat flux) to the most conservative bridge available in the code (the flux is assessed using a reciprocal approach similar to the addition of resistances in parallel). This was applied consistently to all the SAMj calculations. To assess this, compound vehicles with more than one connected component were heated using the reciprocal bridge in order to maintain the fragmentation profile, but single-component objects were heated using the minimum bridge. This resulted in the number of landed objects in SAMj becoming very close to that predicted by DRAMA. This suggests that some effort should be placed into the understanding of the aerothermodyamic heating in the rarefied regime. This is of particular importance given both the sensitivity to the model shown here, and the major fragmentation events in an uncontrolled re-entry occurring in rarefied flow.

A significant benefit of the probabilistic approach is that an assessment of the probability distributions for the landed mass and the landed fragment number can be made. This is performed here via plotting of the centiles of landed mass and landed fragment number, as shown in Figs. 15 and 16.

The agreement in the landed mass across the simulations can be seen to be excellent for AstroBus and BeppoSax. For Sentinel-1 and Sentinel-2, SAMj predicts a lower landed mass. This is driven by the CFRP objects in the Sentinel-2 case, and in the Sentinel-1 case SAMj demises significantly more of the SAR panel mass. The trends can be seen to be in excellent agreement in all cases. This serves to provide significant confidence that the behaviour of the tools is consistent, even when the results from a single simulation may differ. This is encouraging given the same spacecraft models are being used, the material models are consistent and the heating algorithms are reasonably similar.

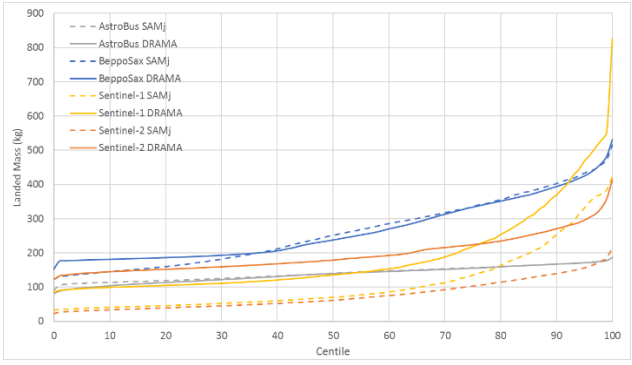

Figure 15. Centiles of Landed Mass for Uncontrolled Re-entry Cases

The landed fragment number plot is more complex. Here, a set of jumps in the profiles can be observed. These occur when sets of fragments shift from being demised to surviving in different Monte Carlo runs. For Sentinel-1, the point at which the SAR panel begins to land fragments can clearly be seen to be around the 50th centile in SAMj, but is between the 60th and 70th centile in

DRAMA. This demonstrates why SAMj lands a higher mean number of fragments. This plot also shown the general trend for SAMj to predict a higher number of landed fragments than DRAMA.

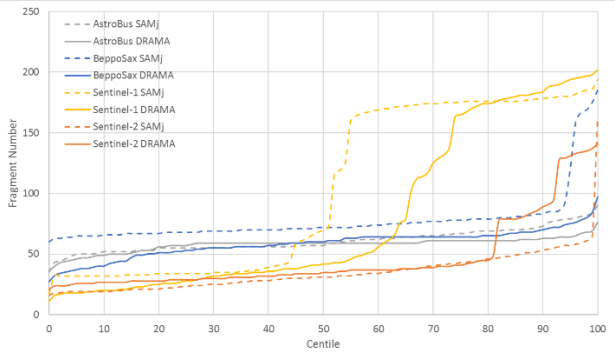

Figure 16. Centiles of Landed Fragment Number for Uncontrolled Re-entry Cases

These centile plots are also helpful in demonstrating the wide range of outcomes which can be predicted within the bounds of the uncertainty model.

The overall agreement between the tools is significantly better than had been expected. A large part of this is the consistent vehicle modelling applied. This suggests that a clear set of rule-based modelling guidelines are required in order to minimize the impact of the specific user on the risk assessment results. ESA has begun this process with the issue of a set of demise verification guidelines, known as DIVE [9].

6 CONCLUSIONS

A large simulation campaign has been performed using a probabilistic approach. Four spacecraft, four re-entry types and two different re-entry tools have been assessed using the PADRE probabilistic re-entry framework. The use of a common input format for the two tools, and a common materials database has demonstrated that, although there are differences in the results from the tools, the overall agreement is good.

The assessment of the tools' performance has been enhanced by the statistical nature of the comparison, and significantly more insight has been obtained than is gained from running a nominal case.

In general, the results show that SAMj lands less mass, but DRAMA lands fewer objects. Interestingly, the landed object number difference is reduced significantly when SAM is reverted to the original, less conservative aerothermodynamic heating bridging function. This has highlighted the heating in the rarefied flow regime as critical to both the fragmentation and demise processes of a spacecraft re-entering from a decaying circular orbit.

7 REFERENCES

[1] T. Lips, "Equivalent re-entry breakup altitude and fragment list", *6th European Conference on Space Debris*, Darmstadt, 2013.

[2] S. Lemmens, et al. "Order of magnitude analysis for on-ground risk from uncontrolled re-entries", Clean Space Industrial Days, Noordwijk, 2016.

[3] M. Balat-Pichelin, P. Omaly, "Study of the atmospheric entry of metallic space debris – oxidation and emissivity evaluation to contribute to "design for demise", *8th European Symposium for Aerothermodynamics of Space Vehicles*, Lisbon, 2015.

[4] G. Parnaby, J. Merrifield, "Synthesis of test results for the identification of key mechanisms for material demise", FGE report CR093/16, 2016.

[5] J. Beck et al. "Improved representation of destructive spacecraft re-entry from analysis of high enthalpy wind tunnel tests of spacecraft equipment", *Acta Astronautica*, v.164, pp. 287-296, 2019.

[6] J. Beck et al, "Progress in probabilistic assessment of destructive re-entry", *1st International Conference on Flight Vehicles, Aerothermodynamics and Re-entry missions*, Monopoli, 2019.

[7] J. Beck, T. Schleutker, A. Caiazzo, T.Soares, "Plasma wind tunnel demisability testing of spacecraft equipment", *1st International Conference on Flight Vehicles, Aerothermodynamics and Re-entry missions*, Monopoli, 2019.

[8] M. Fittock et al., "Methodology and results of high enthalpy wind tunnel and static demisability testing for existing spacecraft structural joining technologies", 69th *International Astronautical Congress*, Bremen, 2018.

[9] ESA, "DIVE – Guidelines for testing and analysing the demise of man made space objects during re-entry", ESA-TECSYE-TN-018311, 2019.

[10] J. Beck, I. Holbrough, J. Merrifield, S. Bainbridge, "Progress in hybrid spacecraft/object oriented destructive re-entry modelling using the SAM code", *7th European Conference on Space Debris*, Darmstadt, 2017.

[11] I. Fuentes et al. "Upgrade of ESA's debris risk assessment and mitigation analysis (DRAMA) tool: spacecraft entry survival analysis module, 6th *European Conference for Aeronautics and Space Science (EUCASS)*, Krakow, 2015.

[12] N. Leveque et al, "Multi-disciplinary assessment of design for demise techniques", D4D-RP-ADSS-SY-1000002584, ESA Final Report, 2017.

[13] G. Koppenwallner, B. Fritsche, T. Lips, "Survivability and ground risk potential of screws and bolts of disintegrating spacecraft during uncontrolled re-entry", *3rd European Conference on Space Debris*, Darmstadt, 2001.

[14] C. Martin et al., "Debris risk assessment and mitigation analysis (DRAMA) tool, ESA Final Report, 2005.